Japanese Journal of Applied Physics
Vol. 44, No. 10, 2005, pp. 7305–7308

Heating Layer of Diamond-Like Carbon Films Used for Crystallization of Silicon Films

Toshiyuki SAMESHIMA and Nobuyuki ANDOH

Tokyo University of Agriculture and Technology, 2-24-16 Naka-cho, Koganei, Tokyo 184-8588, Japan

(Received May 22, 2005; accepted June 25, 2005; published October 11, 2005)

Rapid thermal crystallization of silicon films with a heating layer of diamond-like carbon (DLC) films is reported. DLC films 200 nm thick have an optical absorbance higher that 0.7 for wavelengths shorter than 1000 nm. They are also heat resistant to about 5000 K. A crystalline volume ratio of 0.85 is achieved for silicon films through heat diffusion from DLC heated by 30-ns-pulsed XeCl excimer laser irradiation at 200 mJ/cm^2 for 100 nm DLC/5 nm SiO_2/25 nm Si/quartz, while it is only 0.4 for 25 nm Si/quartz because of high reflection loss. Crystallization of silicon films is also achieved by 1064 nm YAG laser heating of the 200 nm DLC layer overlying the silicon films. [DOI: 10.1143/JJAP.44.7305]

KEYWORDS: crystallization, optical absorbance, rapid thermal heating, DLC

1. Introduction

Low temperature processing technologies allow us to use inexpensive substrates, such as glass substrates, for fabricating thin film transistors (TFTs).[1–3] Laser crystallization processes using the XeCl excimer laser have been widely used to reduce the processing temperature of TFTs.[4–7] The high absorption coefficient of silicon films, $\sim 10^6$ cm^{-1} at 308 nm, is attractive for the absorption the laser light. However reflection loss is serious because of high optical reflectivity of silicon, ~60% at 308 nm. On the other hand, silicon has low optical absorption coefficients in visible and infrared regions because of its indirect band structure.

In this paper, we report pulsed-laser-induced crystallization of silicon films using diamond-like carbon (DLC) as a heating source. We show high optical absorbances for wavelengths shorter than 1000 nm and a high heat resistance of DLC films. We report the effective crystallization of silicon films with a high crystalline volume ratio by laser irradiation with a low energy density.

2. Experimental

DLC films with thicknesses of 100 and 200 nm were formed on quartz substrates at room temperature by a plasma-sputtering method with a carbon target.[8] For structural analyses of the DLC films, Raman scattering spectral measurements were carried out using a 532 nm excitation laser. Optical transmissivity and reflectivity spectra as a function of wavelength from 250 to 1100 nm were measured. Spectroscopic ellipsometry was also used between 250 and 700 nm to analyze the optical properties of DLC films. A 30-ns-pulsed 308 nm XeCl excimer laser was irradiated onto the DLC films in vacuum at room temperature in order to investigate their heat resistance.

For laser crystallization of silicon films, 25 nm and 50-nm-thick amorphous silicon films were formed on quartz substrates by the plasma sputtering method. Then 5-nm-thick SiO_2 films followed by DLC films with thicknesses of 100 and 200 nm were subsequently formed on the silicon films. A 308 nm XeCl excimer laser and 1064 nm Nd^+ YAG laser were irradiated onto samples of DLC/SiO_2/Si/quartz at room temperature. Oxygen plasma treatment was used to remove the DLC films. Raman scattering and optical reflectivity spectra were measured for structural analysis of silicon films. Si films/quartz samples were also irradiated with the lasers for comparison.

3. Results and Discussion

Figure 1 shows Raman scattering spectra for 200-nm-thick DLC films formed on quartz substrates. There were two important peaks; the *D* band at 1360 cm^{-1} associated with sp^3-bond vibration and the *G* band at 1590 cm^{-1} associated with disordered sp^2-bond vibration,[9] as shown in Fig. 1. Spectral analysis using Gaussian curves revealed that the *D* band is a broad band with a full width at half maximum (FWHM) of 333 cm^{-1}, and that *G* band has FWHM of 141 cm^{-1}. There is no significant change in the Raman spectra obtained by 5-shot irradiation with the XeCl excimer laser in vacuum at 350 and 500 mJ/cm^2. This result suggests that carbon bonding properties were negligibly changed upon rapid heating with the XeCl excimer laser.

Figure 2 shows transmissivity spectra (a) and reflectivity spectra (b) as a function of wavelength for DLC films with thicknesses of 100 and 200 nm. Low transmissivity and low reflectivity were observed for wavelengths from 250 to 1100 nm. The transmissivity decreased as the wavelength decreased. In particular, it was lower than 0.11 for wavelengths shorter than 1100 nm for 200-nm-thick DLC films. The reflectivity also decreased as the wavelength decreased. It was lower than 0.2 for wavelengths shorter than 1100 nm for 200-nm-thick DLC films. There were no changes in the optical transmissivity or reflectivity after laser irradiation with the energy density of 350 mJ/cm^2 for 5 shots. The initial smooth surface also remained after the laser irradiation. Figure 3 shows the refractive index and extinction coefficient spectra from 250 to 1100 nm for DLC films

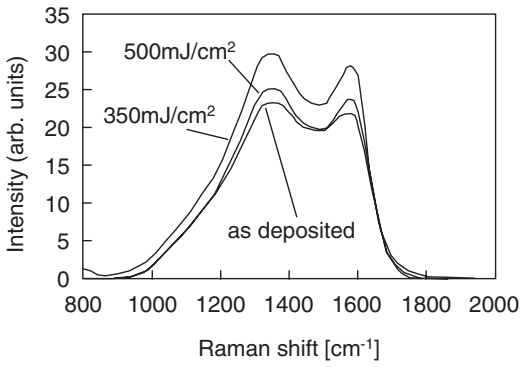

Fig. 1. Raman scattering spectra for 200-nm-thick DLC films formed on quartz substrates. They were as-fabricated and irradiated with XeCl excimer laser in vacuum at 350 and 500 mJ/cm^2.

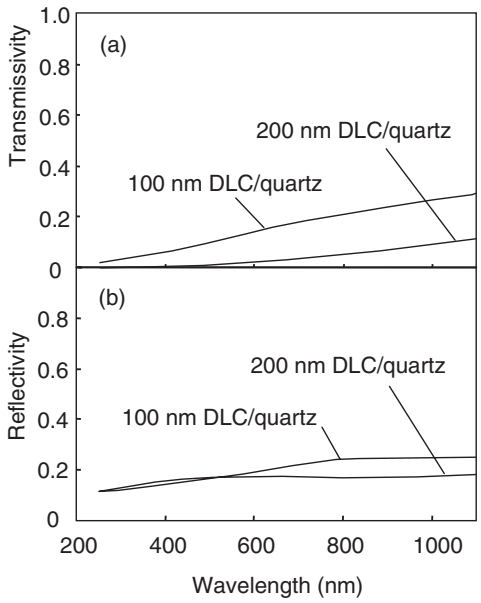

Fig. 2. Transmissivity spectra (a) and reflectivity spectra (b) as a function of wavelength for DLC films with thicknesses of 100 and 200 nm.

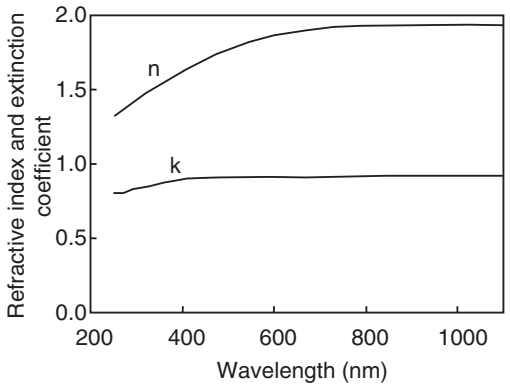

Fig. 3. Refractive index and extinction coefficient spectra as a function of wavelength for DLC films, obtained from the optical transmissivity and reflectivity spectra as well as spectroscopic ellipsometry spectra.

obtained from the optical transmissivity and reflectivity spectra, as well as the spectroscopic ellipsometry spectra. The DLC films had a low refractive index from 1.3 to 1.9 and a high extinction coefficient from 0.8 to 0.9 for wavelengths from 250 to 1100 nm. The low optical reflectivity shown in Fig. 2(b) results from the low refractive index. The extinction coefficients from 0.8 to 0.9 give high optical absorption coefficients from 1.0×10^5 to 3.0×10^5 cm^{-1} as the wavelength decreases from 1100 to 250 nm. These results indicate that DLC films act as the optical absorption layer. Using the data of optical reflectivity and optical absorption, numerical heat flow calculation by the finite-element method was conducted for the case of 30-ns-pulsed XeCl excimer laser irradiation of 100-nm-thick DLC films on quartz glass substrates. Figure 4 shows the temperature distribution in the depth direction with different laser energies at 30 ns from the laser initiation, at which the DLC films were heated to the highest temperature with each laser irradiation. The calculation included heat diffusion into air

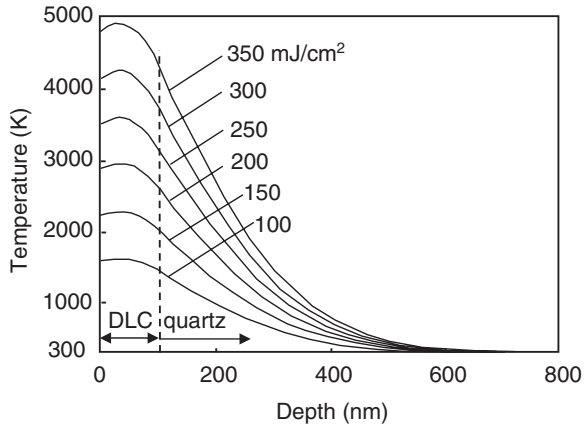

Fig. 4. Calculated temperature distribution in the depth direction with different laser energies at 30 ns.

as well as to quartz substrates. The carbon surface was rapidly heated by laser irradiation because the heat diffusivity of quartz is low and heat energy was kept at the surface during laser irradiation. The maximum temperature appeared in the DLC films slightly below the top surface because of the heat diffusion into air. Temperature increased to 1600 K in the DLC films and it increased to 1500 K at the DLC/quartz interface for laser irradiation at 100 mJ/cm^2. The calculated peak temperatures in the DLC film and DLC/quartz interface increased to 4800 and 4300 K, respectively, for laser irradiation at 350 mJ/cm^2. In the numerical heat flow calculation, we used the low optical reflectivity at 308 nm as shown in Fig. 2(b). We assumed that the reflectivity did not change with the temperature of the DLC layers and that laser energy was effectively incorporated into DLC layers. Moreover, in the numerical heat flow calculation, we did not consider heat dissipation by convection of air and cooling by wind caused by the high temperature gradient near the DLC surface. Although these uncertain factors can cause the calculated temperature of samples to be low, the results of calculated in-depth temperature distribution shown in Fig. 4 indicate that there is a possibility of heating silicon to sufficiently above the melting temperature of silicon (1685 K) through heat diffusion from DLC layers heated by laser irradiation at a low energy density when the DLC layer is formed on the silicon films.

Figure 5 shows the calculated optical absorbance of samples for DLC/25 nm Si/quartz with different thicknesses of DLC as a function of wavelength. The numerical calculation was conducted using complex fresnel coefficients for the multilayered structure.[10] The formation of 100-nm-thick DLC films resulted in an optical absorbance of 0.86 at 308 nm because of the high optical absorption coefficient and the low optical reflectivity, while it was only 0.41 for 25 nm a-Si/quartz. Although the optical absorbance was 0.31 at 1064 nm for the case of 100 nm DLC/25 nm Si/quartz, it increased to 0.74 as the thickness of DLC increased to 200 nm. It was 0.81 for the case of the 500-nm-thick DLC coating. On the other hand, there was almost no optical absorbance at 1064 nm for 25 nm a-Si/quartz because of the low optical absorption coefficient of silicon. These results shown in Figs. 1–5 indicate that the DLC heating layer had

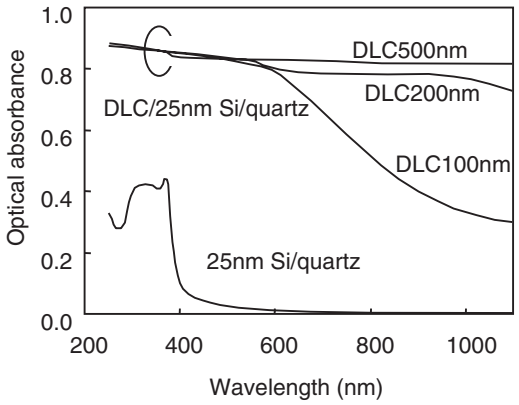

Fig. 5. Calculated optical absorbance of samples for DLC/25 nm Si/quartz with different thicknesses of DLC as a function of wavelength.

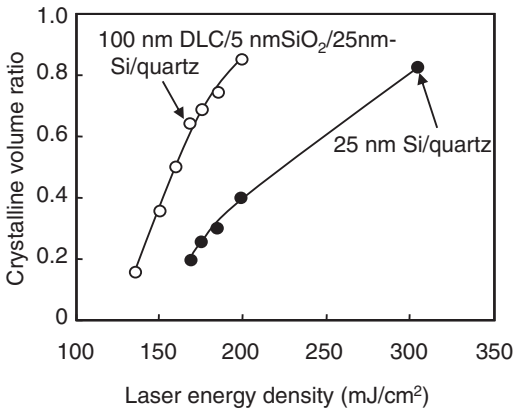

Fig. 7. Crystalline volume ratio of poly-Si obtained by analyzing of optical reflectivity spectra in the ultraviolet region, as a function of laser energy density.

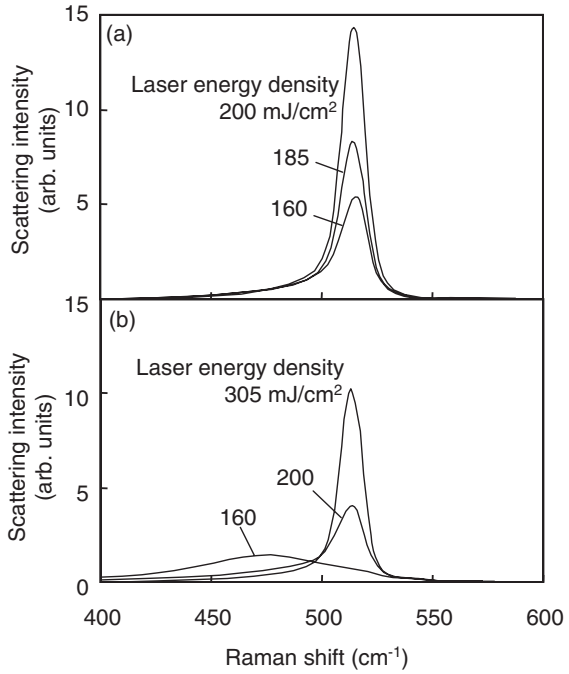

Fig. 6. Raman scattering spectra of silicon films 100 nm DLC/5 nm SiO_2/25 nm Si/quartz (a) and 25 nm Si/quartz (b) when the samples were irradiated with XeCl excimer laser with different energy densities.

the good properties of high optical absorption and heat resistance required to crystallize silicon films.

Figure 6 shows Raman scattering spectra of silicon films for 100 nm DLC/5 nm SiO_2/25 nm Si/quartz (a) and 25 nm Si/quartz (b) when the samples were irradiated with the XeCl excimer laser. A high and sharp phonon band of crystalline silicon was observed with laser irradiation at 160 mJ/cm^2 for the samples of 100 nm DLC/5 nm SiO_2/25 nm Si/quartz, The Raman scattering measurement was carried out after removing DLC films by oxygen plasma etching. The intensity of the phonon band increased as the laser energy density increased to 200 mJ/cm^2, as shown in Fig. 6(a). On the other hand, there was no crystalline phonon band for laser irradiation at 160 mJ/cm^2 for 25 nm Si/quartz as shown in Fig. 6(b), because the laser energy was just below the crystallization threshold for the Si/quartz structure. The intensity of the crystalline phonon band was very low with 200 mJ/cm^2 laser irradiation for Si/quartz. An energy density of 305 mJ/cm^2 was necessary in order to form crystalline silicon with a phonon intensity comparable to that of 100 nm DLC/5 nm SiO_2/25 nm Si/quartz formed at 200 mJ/cm^2, as shown in Fig. 6(b). Figure 7 shows the crystalline volume ratio, obtained by analyzing optical reflectivity spectra in the ultraviolet region as a function of laser energy density.[11] For the analysis of the crystalline volume ratio, we used the peak around 276 nm (E_2 peak), which was caused by the large joint density of states at the *X* point in the Brillouin zone of crystalline silicon, while there was no peak for amorphous silicon. We calculated the optical reflectivity spectra of poly-Si films using a program taking account surface roughness and optical interference effects. The complex refractive index of poly-Si ($n_{\text{poly-Si}}$) was assumed to be a combination of the complex refractive indexes of crystalline silicon films ($n_{\text{c-Si}}$) and amorphous silicon films ($n_{\text{a-Si}}$);

$$n_{\text{poly-Si}} = Cn_{\text{c-Si}} + (1 - C)n_{\text{a-Si}} \quad (1)$$

where *C* is the crystalline volume ratio. The most probable crystalline volume ratio was determined from the best fit of optical reflectivity spectra to the experimental ones using the calculated complex refractive index of polycrystalline silicon given by eq. (1). Crystallization was observed with laser energy above 135 mJ/cm^2 for 100 nm DLC/5 nm SiO_2/25 nm Si/quartz, although the crystallization threshold was 170 mJ/cm^2 for 25 nm Si/quartz, as shown in Fig. 7. The crystalline volume ratio of the silicon films for 100 nm DLC/5 nm SiO_2/25 nm Si/quartz was higher than that for 25 nm Si/quartz in the case of laser energy. It was 0.85 at 200 mJ/cm^2 for 100 nm DLC/5 nm SiO_2/25 nm Si/quartz, while it was only 0.4 in the case of 25 nm Si/quartz, as shown in Fig. 7. An laser energy density of 305 mJ/cm^2 was needed to crystallize silicon films with a crystalline volume ratio above 0.8 for the 25 nm Si/quartz structure. The results in Figs. 6 and 7 revealed that the 25-nm-thick silicon films were well crystallized with the low laser energy density of 200 mJ/cm^2 when the DLC heating layer was used. The DLC films effectively absorbed the laser light and were heated to high temperature. The heat energy effectively diffused into underlying silicon films and caused crystallization of silicon films. Because the silicon films were

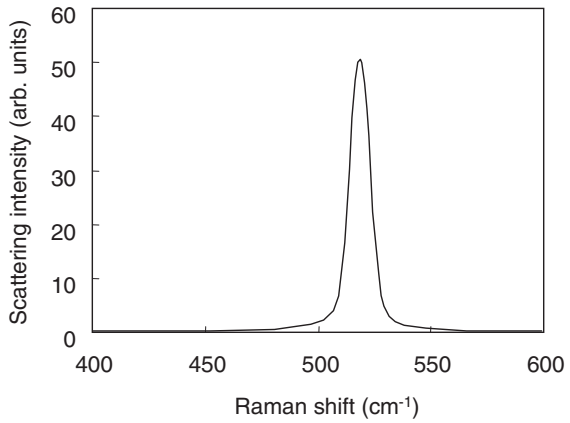

Fig. 8. Raman scattering spectra of silicon films for 100 nm DLC/5 nm SiO_2/50 nm Si/quartz when the samples were irradiated with 1064 nm YAG laser with an intensity of 4 kW/cm^2 for 5 ms.

placed in 100 nm deep from the top surface, the temperature at the surface region must be increased to much higher than the melting point of silicon, 1685 K when the silicon films are crystallized. High heat resistance of DLC about 5000 K is suitable for the heating layer.

Figure 8 shows Raman scattering spectra of silicon films for 200 nm DLC/5 nm SiO_2/50 nm Si/quartz when the samples were irradiated with the 1064 nm YAG laser with an intensity of 4 kW/cm^2 for 5 ms. A high scattering intensity and a sharp crystalline phonon band were observed. There was no residual amorphous band. This means that the silicon films were completely crystallized by heat diffusion from the DLC top layer that was heated by YAG laser irradiation. On the other hand, no crystallization was observed in the case of YAG laser irradiation to 50 nm Si/quartz at 4 kW/cm^2 for 5 ms because there was no absorption of silicon films.

4. Summary

Rapid thermal crystallization of thin silicon films with a heating layer of diamond-like carbon (DLC) films formed by sputtering was discussed. DLC films had low refractive indices from 1.3 to 1.9 and high extinction coefficients from 0.8 to 0.9 for wavelengths from 250 to 1100 nm. These properties resulted in optical absorbance higher than 0.7 for 200-nm-thick DLC films for wavelengths shorter than 1000 nm. The numerical heat flow calculation suggested a high heat resistance to about 5000 K. The silicon films were crystallized well upon irradiation with a 30 ns XeCl excimer laser at 200 mJ/cm^2 when 100-nm-thick DLC films were coated on the silicon films. A crystalline volume ratio of 0.85 of silicon films was achieved. Heat diffusion from DLC heated by 30-ns-pulsed XeCl excimer laser irradiation effectively crystallized the underlying silicon films. On the other hand, the crystalline volume ratio was only 0.4 for laser irradiation of 25 nm Si/quartz at 200 mJ/cm^2 because of a high reflection loss of 0.6 at the silicon surface. Crystallization of silicon films was also achieved by 1064 nm YAG laser irradiation using a 200 nm DLC heating layer. Silicon films were completely crystallized by heat diffusion from the DLC films heated by the YAG laser.

Acknowledgment

We thank Dr. S. Hirono for his support.

1) S. Uchikoga and N. Ibaraki: Thin Solid Films **383** (2001) 19.
2) S. Inoue, K. Sadao, T. Ozawa, Y. Kobashi, H. Kwai, T. Kitagawa and T. Shimoda: Tech. Dig. IEDM, 2000, p. 197.
3) K. Shibata and H. Takahashi: Proc. Int. Workshop on Active Matrix Liquid Crystal Displays'01, 2001, p. 219.
4) T. Sameshima, S. Usui and M. Sekiya: IEEE Electron Device Lett. **7** (1986) 276.
5) K. Sera, F. Okumura, H. Uchida, S. Itoh, S. Kaneko and K. Hotta: IEEE Trans. Electron Devices **36** (1989) 2868.
6) T. Serikawa, S. Shirai, A. Okamoto and S. Suyama: Jpn. J. Appl. Phys. **28** (1989) L1871.
7) A. Kohno, T. Sameshima, N. Sano, M. Sekiya and M. Hara: IEEE Trans. Electron Devices **42** (1995) 251.
8) T. Sameshima and N. Andoh: Proc. Mater. Res. Soc. Symp. **358** (2004) KK9.5.
9) M. Yoshikawa, N. Nagai, M. Matsuki, H. Fukada, G. Katagiri, H. Ishida, A. Ishitani and I. Nagai: Phys. Rev. B **46** (1992) 7169.
10) M. Born and E. Wolf: *Principles of Optics* (Pergamon, New York, 1974) Chaps. 1 and 13.
11) T. Sameshima, N. Andoh and Y. Andoh: Jpn. J. Appl. Phys. **44** (2005) 1186.